

Boundary Element Modeling of Pyroelectric Solids with Shell Inclusions

Heorhiy SULYM
h.sulym@pb.edu.pl

*Bialystok University of Technology
Wiejska Str. 45C, 15-351 Bialystok, Poland*

Iaroslav PASTERNAK
Viktoriya PASTERNAK

*Lutsk National Technical University
Lvivska Str. 75, 43018 Lutsk, Ukraine*

Received (18 July 2018)
Revised (27 August 2018)
Accepted (21 October 2018)

The paper presents general boundary element approach for analysis of thermoelectroelastic (pyroelectric) solids containing shell-like electricity conducting permittive inclusions. The latter are modeled with opened surfaces with certain boundary conditions on their faces. Rigid displacement and rotation, along with constant electric potential of inclusions are accounted for in these boundary conditions. Formulated boundary value problem is reduced to a system of singular boundary integral equations, which is solved numerically by the boundary element method. Special attention is paid to the field singularity at the front line of a shell-like inclusion. Special shape functions are introduced, which account for this square-root singularity and allow accurate determination of field intensity factors. Numerical examples are presented.

Keywords: pyroelectric, anisotropic, rigid shell-like inclusion, field intensity factor.

1. Introduction

Nowadays thermoelectroelastic (pyroelectric) materials and smart structures are widely used in modern technologies, since they allow monitoring of internal state and self-tuning, serve as sensors and actuators, positioning devices etc. These useful features of such materials are due to the ability of coupling of mechanical, electric and thermal fields, which is caused by internal structure of the material (molecular or composite). There is wide range of experimental and theoretical studies of pyroelectric materials and their applications [1]. Particular interest is paid to fracture of piezoelectric solids [2] under the action of mechanical and electric loading.

The boundary element method (BEM) is one of the most prospective approaches

in fracture mechanics analysis, since it requires only boundary mesh and allows obtaining very accurate values of field intensity factors due to simple accounting for square-root singularity. A number of works address 3D fracture mechanics under piezoelectric, piezomagnetic and magnetoelastoelectric coupling. Furthermore, there exists another class of field concentrators, which has similar square-root singularity on its front and is commonly referred as an anti-crack or a rigid shell inclusion. Such inhomogeneities can model internal electrodes, which control or inform about the state of a smart solid. There are not so much publications concerning anti-cracks in anisotropic solids comparing to crack problems. Fabrikant [3] et al. provided the analysis of transversely-isotropic half-space containing a crack or inclusion under the action of a rigid punch. Kaczyński and Kozłowski [4] studied thermal stress in elastic medium containing flat rigid inclusion. Kaczyński [5, 6] and Kaczyński & Kaczyński [7] extended these results to transversely isotropic and pyroelectric medium. Kirilyuk [8] provided the analysis of a penny-shaped crack opened by rigid inclusion.

Nevertheless, to the best of authors' knowledge there are no publications considering non-flat rigid shell-like inclusions in pyroelectric solids. Another issues arising considering rigid inclusions is their ability to move and rotate, which is not always accounted for in the anti-crack boundary conditions. Therefore, this paper is focused on the development of a solid boundary element approach for analysis of field intensity caused by rigid electricity-conducting shell-like inclusions of arbitrary smooth shape.

2. Governing equations of heat conduction and thermoelectroelasticity

According to [9], in a fixed Cartesian coordinate system $Ox_1x_2x_3$ the equilibrium equations, the Maxwell equations (Gauss theorem for electric and magnetic fields), and the balance equations of heat conduction in the steady-state case can be presented in the following compact form:

$$\tilde{\sigma}_{Ij,j} + \tilde{f}_I = 0 \quad h_{i,i} - f_h = 0 \quad (1)$$

where the capital index varies from 1 to 4, while the lower case index varies from 1 to 3, i.e. $I = 1, 2, 3, 4$. $i = 1, 2, 3$. Here and further the Einstein summation convention is used. A comma at subscript denotes differentiation with respect to a coordinate indexed after the comma, i.e. $u_{i,j} = \partial u_i / \partial x_j$.

In the assumption of small strains and fields' strengths the constitutive equations of linear thermoelectroelasticity in the compact notations are as follows [9]:

$$\tilde{\sigma}_{Ij} = \tilde{C}_{IjK m} \tilde{u}_{K,m} - \tilde{\beta}_{Ij} \theta, \quad h_i = -k_{ij} \theta_{,j} \quad (2)$$

where:

$$\begin{aligned} \tilde{u}_i &= u_i, \quad \tilde{u}_4 = \phi, \quad \tilde{u}_5 = \psi; \quad \tilde{f}_i = f_i, \quad \tilde{f}_4 = -q \\ \tilde{\sigma}_{ij} &= \sigma_{ij}, \quad \tilde{\sigma}_{4j} = D_j \\ \tilde{C}_{ijklm} &= C_{ijklm}, \quad \tilde{C}_{ij4m} = e_{mij}, \quad \tilde{C}_{4jkm} = e_{jkm}, \quad \tilde{C}_{4j4m} = -\kappa_{jm} \\ \tilde{\beta}_{ij} &= \beta_{ij}, \quad \tilde{\beta}_{4j} = -\chi_j \quad (i, j, k, m = 1, 2, 3) \end{aligned} \quad (3)$$

σ_{ij} is a stress tensor; f_i is a body force vector; D_i is an electric displacement vector; q is a free charge volume density; h_i is a heat flux; f_h is a distributed

heat source density; u_i is a displacement vector; ϕ is an electric potential; θ is a temperature change with respect to the reference temperature; C_{ijkl} are the elastic stiffnesses (elastic moduli); k_{ij} are heat conduction coefficients; e_{ijk} are piezoelectric constants; κ_{ij} are dielectric permittivities; β_{ij} , χ_i are thermal moduli and pyroelectric coefficients, respectively.

Thus, the problem of linear thermoelectroelasticity is to solve partial differential equations (1) and (2) under the given boundary conditions and volume loading. Since electro-mechanical fields do not influence temperature field in the considered problem (uncoupled thermoelectroelasticity) the first step is to solve the heat conduction equation and the second one is to determine mechanical and electric fields acting in the solid.

3. Problem formulation and boundary integral equations

Consider a pyroelectric solid B containing smooth shell-like rigid electricity conducting inclusions S_k ($k = 1, \dots, n$) (Fig. 1). The latter can be either thermally insulated or perfectly heat conductive. It is assumed that inclusions are perfectly bonded with the medium. On the surface ∂B of the solid B either type I (heat flux, stress, electric displacement), or type II (temperature, displacement, electric potential) or mixed boundary conditions are given. Volume loading can be also present.

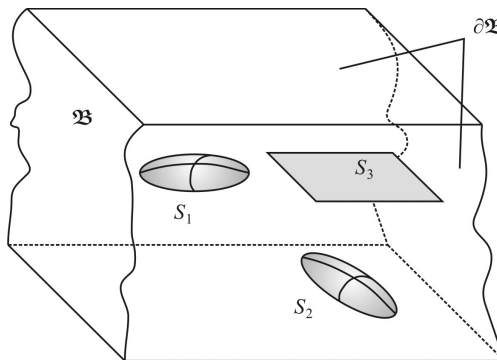


Figure 1 The sketch of the problem

First consider boundary conditions at surfaces S_k of the medium, which model shell-like rigid inclusions. Since uncoupled thermoelectroelasticity is considered, heat conduction boundary conditions can be considered independently of pyroelectric ones.

In the case of thermally insulated inclusions heat flux is zero at their faces, thus accounting for the perfect bonding of inclusions boundary conditions at surfaces S_k can be written as:

$$\Sigma h_n(x_0) = 0, \quad \Delta h_n(x_0) = 0 \quad \forall x_0 \in S_k \tag{4}$$

where $\Sigma f = f^+ + f^-$; $\Delta f = f^+ - f^-$; $h_n = h_i n_i$; $\Sigma h_n = h_i^+ n_i^+ + h_i^- n_i^- = (h_i^+ - h_i^-) n_i^+$; $n^+(x) = -n^-(x)$ are unit outwards normal vectors to the faces S_k^+ and S_k^- of the mathematical cut S_k (slit surface S_k inside a solid \mathbf{B}); boundary values denoted with superscripts “+” and “-” corresponds to appropriate faces.

In the case of perfectly heat conductive inclusions it is assumed that their temperatures are constant, therefore, boundary conditions on S_k^+ and S_k^- write as:

$$\Delta\theta(x_0) = 0, \quad \frac{1}{2}\Sigma\theta(x_0^k) = \theta_k^0 \quad \forall x_0^k \in S_k \quad (k = 1, \dots, n) \quad (5)$$

where θ_k^0 is a temperature of the k -th inclusion. Additionally inclusion can generate or absorb heat, which can be mathematically written through their heat balance equations as:

$$\iint_{S_k} \Sigma h_n(x) dS(x) - H_0^k = 0 \quad (k = 1, \dots, n) \quad (6)$$

where H_0^k is the constant heat (actually heat generation rate) applied to the k -th inclusion. The minus sign in Eq. (6) is due to the contact conditions, since h_n on the inclusion is opposite to those on a medium.

Since rigid inclusions considered are not fixed, the displacements at surfaces S_k are given through the following kinematic equations:

$$\frac{1}{2}\Sigma u_i(x^k) = u_i^k + \varepsilon_{ijm} \omega_j^k x_m^k, \quad \Delta u_i(x^k) = 0 \quad \forall x^k \in S_k \quad (k = 1, \dots, n) \quad (7)$$

where u_i^k is a rigid displacement of the k -th inclusion and ω_j^k is its rigid rotation about the origin; ε_{ijm} is the permutation tensor.

Electric potential is assumed to be constant to model electrostatics of electricity-conducting inclusion:

$$\frac{1}{2}\Sigma\phi(x^k) = \phi_0^k, \quad \Delta\phi(x^k) = 0 \quad \forall x^k \in S_k \quad (k = 1, \dots, n) \quad (8)$$

where ϕ_0^k is an electric potential of the k -th inclusion.

Introducing extended permutation tensor $\tilde{\varepsilon}_{Ijm}$, which equals to permutation tensor if $I \leq 3$ and is zero otherwise:

$$\tilde{\varepsilon}_{Ijm} = \begin{cases} \varepsilon_{Ijm} & I \leq 3 \\ 0 & \text{otherwise} \end{cases} \quad (9)$$

one can reduce Eqs. (7) and (8) to the following compact form:

$$\frac{1}{2}\Sigma\tilde{u}_I(x^k) = \tilde{u}_I^k + \tilde{\varepsilon}_{Ijm} \omega_j^k x_m^k, \quad \Delta\tilde{u}_I(x^k) = 0 \quad \forall x^k \in S_k \quad (k = 1, \dots, n) \quad (10)$$

where \tilde{u}_I^k are unknown extended displacements of the k -th inclusion.

Additionally inclusions can be loaded with some extended forces and couples. Therefore, their models should be accompanied with equilibrium equations, which write as:

$$\iint_{S_k} \Sigma\tilde{t}_I(x) dS(x) - \tilde{P}_I^k = 0 \quad (11)$$

$$\iint_{S_k} \varepsilon_{ijm} x_j \Sigma t_m(x) dS(x) - M_i^k = 0 \quad (k = 1, \dots, n) \quad (12)$$

where \tilde{P}_I^k and M_i^k are extended forces and couples applied to the k -th inclusion, respectively.

According to [9], solution of partial differential equations (1) and (2) for a solid with a system of internal opened surfaces, on which some boundary conditions are set, is reduced to the following boundary integral equations of heat conduction and thermoelectroelasticity:

$$\begin{aligned} \frac{1}{2} \Sigma \theta(x_0) &= \iint_S \Theta^*(x, x_0) \Sigma h_n(x) dS(x) \\ &\quad - CPV \iint_S H^*(x, x_0) \Delta \theta(x) dS(x) \\ &\quad - \iiint_B \Theta^*(x, x_0) f_h(x) dV(x) \end{aligned} \quad (13)$$

$$\begin{aligned} \frac{1}{2} \Sigma \tilde{u}_I(x_0) &= \iint_S U_{IJ}(x, x_0) \Sigma \tilde{t}_J(x) dS(x) \\ &\quad - CPV \iint_S T_{IJ}(x, x_0) \Delta \tilde{u}_J(x) dS(x) \\ &\quad + \iint_S [R_I(x, x_0) \Delta \theta(x) + V_I(x, x_0) \Sigma h_n(x)] dS(x) \\ &\quad + \iiint_B U_{IJ}(x, x_0) \tilde{f}_J(x) dV(x) - \iiint_B V_I(x, x_0) f_h(x) dV(x) \end{aligned} \quad (14)$$

where $x_0 \in S$; $S = \bigcup_k S_k \cup \partial B$; and $\Sigma \theta = \Delta \theta = \theta$, $\Sigma h_n = \Delta h_n = h_n$, $\Sigma \tilde{u}_I = \Delta \tilde{u}_I = \tilde{u}_I$, $\Sigma \tilde{t}_I = \Delta \tilde{t}_I = \tilde{t}_I$ on ∂B ; CPV stands for the Cauchy Principal Value of the integral. The kernels of Eqs. (13) and (14) are derived in Ref [10].

Thus, the problem is reduced to solution of boundary integral equations (5), (6), (10)–(14) for determination of unknown heat flux and extended stress discontinuities (Σh_n and Σt_I) on surfaces S_k and extended rigid displacements and rotations of inclusions.

However, prior to solution of these equations one should note that in 2D case (plane strain) sought field discontinuities possess square root singularity at inclusion's tip [11]. These results can be naturally extended on 3D case of a rigid shell-like inclusion with a smooth front line of a curvature radius $R_C(A)$, since one can always select some domain surrounding point A (see Fig. 2) in front of the inclusion such that its characteristic size $\varepsilon \ll R_C(A)$, thus one can neglect inclusion's front curvature $1/R_C(A)$, and the solution of the problem can be presented as a superposition of plane strain and out-of-plane strain.

Therefore, according to [11] extended stress field in front of the inclusion in a local coordinate system $A\tau nm \sim Ax_1x_2x_3$ (Fig. 2) is defined as:

$$\begin{aligned} \tilde{\sigma}_1 = [\tilde{\sigma}_{i1}] &= \frac{2}{\sqrt{2\pi}} Im \left\{ B \left\langle p_* Z_*^{-1/2} \right\rangle A^T \tilde{k}^{(2)} \right\} \\ \tilde{\sigma}_2 = [\tilde{\sigma}_{i2}] &= \frac{-2}{\sqrt{2\pi}} Im \left\{ B \left\langle Z_*^{-1/2} \right\rangle A^T \tilde{k}^{(2)} \right\} \end{aligned} \quad (15)$$

where $\langle Z_*^{-1/2} \rangle = \text{diag} [(x_1 + p_1 x_2)^{-1/2}, \dots, (x_1 + p_4 x_2)^{-1/2}]$; matrices A , B and constants p_α ($\alpha = 1, \dots, 4$) are determined from the Stroh eigenvalue problem [12]; and extended field intensity factor vector $\tilde{k}^{(2)} = [K_{12}^{(2)}, K_{22}^{(2)}, K_{32}, K_{42}]^T$ is defined as:

$$\tilde{k}^{(2)} = - \lim_{x \rightarrow x(A)} \sqrt{\frac{\pi s(x)}{2}} \Sigma \tilde{t}(x) \quad (16)$$

Extended stress discontinuity $\Sigma \tilde{t}$ in Eq. (16) is computed in a local coordinate system $A\tau nm \sim Ax_1 x_2 x_3$ (Fig. 2).

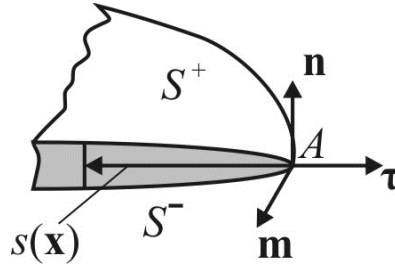


Figure 2 Inclusion's front line

Since according to Eq. (15) local singular extended stress field is completely defined by field intensity factors $\tilde{k}^{(2)}$, the latter are considered as sought values in the solution of formulated problem.

In addition to extended stress field intensity, heat flux also possesses square root singularity, thus heat flux intensity factors are determined through the following relations [9]:

$$K_{h1} = - \lim_{x \rightarrow x(A)} \sqrt{\frac{\pi}{8s(x)}} k_t \Delta \theta(x), \quad K_{h2} = - \lim_{x \rightarrow x(A)} \sqrt{\frac{\pi s(x)}{2}} \Sigma h_n(x) \quad (17)$$

where $k_t = \sqrt{k_{\tau\tau} k_{nn} - k_{\tau n}^2}$; $k_{\tau\tau} = k_{ij} \tau_i \tau_j$, $k_{nn} = k_{ij} n_i n_j$, $k_{\tau n} = k_{ij} \tau_i n_j$.

4. Boundary element solution strategy. Determination of field intensity factors

4.1. Boundary element mesh and special shape functions

For the boundary element solution of derived boundary integral equations for a particular problem the surface ∂B of the solid along with inclusion surfaces S_k are meshed with quadrilateral quadratic discontinuous boundary elements. The local curvilinear coordinate system $O\xi\eta$ is associated with each boundary element, moreover, $-1 \leq \xi \leq 1$, $-1 \leq \eta \leq 1$. The collocation points are placed at nodes $\xi = (-2/3; 0; 2/3)$; $\eta = (-2/3; 0; 2/3)$. Therefore, there are 9 collocation points associated with each boundary element.

Boundary conditions along with unknown boundary and discontinuity functions are interpolated within the collocation points at each boundary element Γ_N as:

$$b_N(\xi, \eta) = \sum_{i=1}^3 \sum_{j=1}^3 b_N^{i,j} \phi_i(\xi) \phi_j(\eta) \tag{18}$$

where $b = (\Delta\theta, \Sigma h_n, \Delta\tilde{u}_I, \Sigma\tilde{t}_I)^T$, and the discontinuous shape functions are given as [13]:

$$\phi_1(\xi) = \xi \left(\frac{9}{8}\xi - \frac{3}{4} \right), \phi_2(\xi) = \left(1 - \frac{3}{2}\xi \right) \left(1 + \frac{3}{2}\xi \right), \phi_3(\xi) = \xi \left(\frac{9}{8}\xi + \frac{3}{4} \right) \tag{19}$$

Special shape functions are used for the heat flux discontinuity function Σh_n and extended stress discontinuity function $\Sigma\tilde{t}_I$ at the inclusion's front boundary elements:

$$\phi_i^\Sigma(\xi) = \frac{1}{\sqrt{1 \pm \xi}} \left(\Phi_{i1}^\Sigma + \sum_{j=2}^3 \Phi_{ij}^\Sigma (1 \pm \xi)^{j-1} \right) \tag{20}$$

which allow to capture square-root singularity (16), (17) arising at inclusion's front line.

Substituting Eqs. (18)–(20) into the boundary integral equations (5), (6), (10)–(14) one obtains the system of linear algebraic equations for unknown nodal values of sought discontinuity functions. Techniques for evaluation of arising regular, weakly and strongly singular integrals are explicitly described in [9].

4.2. Determination of field intensity factors

Consider a local coordinate system at a point A of the inclusion front (Fig. 2). The axes of this system are defined by three unit orthogonal vectors n, m, τ , where n is a normal to inclusion surface; m is a tangent to the inclusion front curve at A , and $\tau = n \times m$. Without loss in generality consider that the boundary element, which the point A belongs to, models inclusion front line with its side $\xi = 1$.

Normal and tangent vectors are defined as:

$$n = \left(\frac{\partial x}{\partial \xi} \times \frac{\partial x}{\partial \eta} \right) / \left| \frac{\partial x}{\partial \xi} \times \frac{\partial x}{\partial \eta} \right|; m = -\frac{\partial x}{\partial \eta} / \left| \frac{\partial x}{\partial \eta} \right| \tag{21}$$

where $x(\xi, \eta)$ is a position vector, which defines the surface of the boundary element. Then according to Eq. (24) the extended traction discontinuity function $\Sigma\tilde{t}^*(x)$ in the local coordinate system $A\tau nm$ on the considered boundary element is equal to:

$$\Sigma\tilde{t}^*(x) = \Omega \sum_{i=1}^3 \sum_{j=1}^3 \Sigma\tilde{t}^{(i,j)} \phi_i^\Sigma(\xi) \phi_j(\eta) \tag{22}$$

where $\Sigma\tilde{t}^{(i,j)}$ are the nodal values of the extended traction discontinuity function, and Ω is the rotation matrix.

Expanding $s(x)$ in Eqs. (16), (17) into Taylor series at the vicinity of A one obtains:

$$s = (1 - \xi) \rho(\eta_A) + O\left((1 - \xi)^2; (\eta_A - \eta)^2 \right) \tag{23}$$

where:

$$\rho(\eta_A) = \tau \cdot \left. \frac{\partial x}{\partial \xi} \right|_{\xi=1, \eta=\eta_A} \quad (24)$$

Substituting (20) and (23) into (16) and evaluating the limit one obtains:

$$\tilde{k}^{(2)} = -\sqrt{\frac{\pi\rho(\eta_A)}{2}} \Omega \sum_{i=1}^3 \sum_{j=1}^3 \Sigma \tilde{t}^{(i,j)} \Phi_{i1}^{\Sigma} \phi_j(\eta_A) \quad (25)$$

which is the formula implemented in the present BEM for precise evaluation of the field intensity factors.

The same way the generalized heat flux intensity factors can be evaluated as:

$$K_{h2} = -\sqrt{\frac{\pi\rho(\eta_A)}{2}} \sum_{i=1}^3 \sum_{j=1}^3 \Sigma h_n^{(i,j)} \Phi_{i1}^{\Sigma} \phi_j(\eta_A) \quad (26)$$

5. Numerical example

Consider a transversely isotropic pyroelectric barium titanate (BaTiO₃), which has the following properties [14]:

- elastic moduli (GPa):
 $C_{11} = C_{22} = 150$; $C_{33} = 146$; $C_{12} = C_{13} = C_{23} = 66$; $C_{44} = C_{55} = 44$;
 $C_{66} = (C_{11} - C_{12})/2 = 42$;
- piezoelectric constants (C/m²):
 $e_{31} = e_{32} = -4.35$; $e_{33} = 17.5$; $e_{15} = e_{24} = 11.4$;
- dielectric constants (nF/m):
 $\kappa_{11} = \kappa_{22} = 9.86775$; $\kappa_{33} = 11.151$;
- heat conduction coefficients (W/(mK)):
 $k_{11} = k_{22} = k_{33} = 2.5$;
- thermal expansion coefficients (K⁻¹):
 $\alpha_{11} = \alpha_{22} = 8.53 \cdot 10^{-6}$; $\alpha_{33} = 1.99 \cdot 10^{-6}$;
- pyroelectric constants (GV/(mK)):
 $\lambda_3 = 13.3 \cdot 10^{-6}$.

The medium contains a shell-like inclusion, which surface is given by the following equation of elliptic paraboloid of revolution:

$$x_3 = \rho (x_1^2 + x_2^2), x_1^2 + x_2^2 \leq R^2 \quad (27)$$

where ρ and R are constants (if $\rho = 0$ one obtains a penny-shaped inclusion of a radius R). Properties of the medium are the same as in the previous subsection.

The inclusion is meshed with only 12 quadrilateral discontinuous boundary elements. Four central boundary elements use general quadratic shape functions (19), while other elements utilize special shape functions (20) to account for the square root singularity of stress and heat flux at the inclusion front.

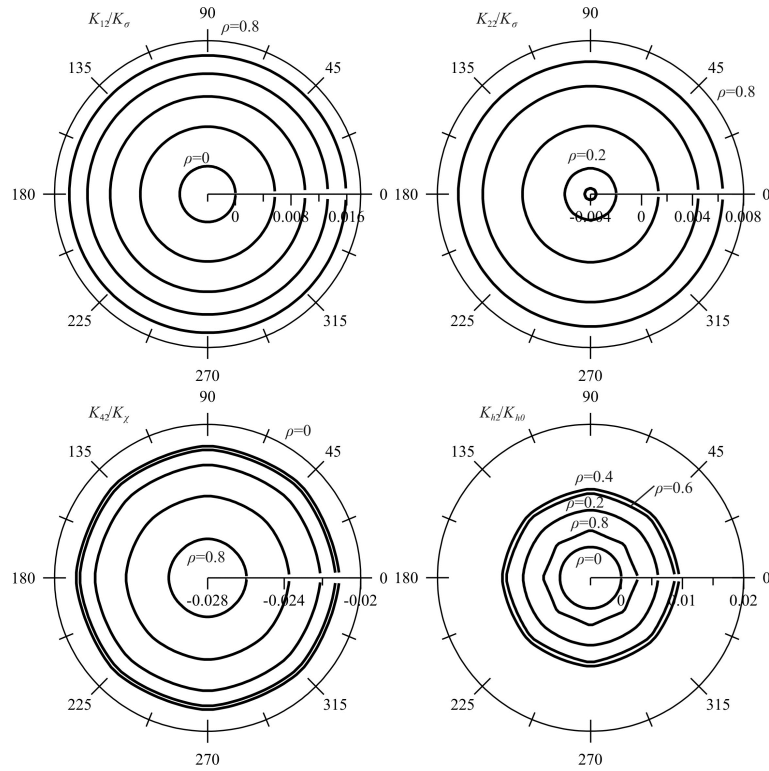


Figure 3 Field intensity factors on the front line of the inclusion

Since due to tertiary pyroelectricity [15] uniform heat flow can produce unbounded stress in infinite pyroelectric solid, the examples presented in [7] are not considered here, because they require additional studies. In turn, in this example the medium is loaded with two point heat sources H_0 and $-H_0$ placed at the points $x_1 = (0; 0; R)^T$ and $x_2 = (0; 0; -R)^T$, respectively. Thus, the volume integrals in Eqs. (13), (14) reduce to:

$$\iiint_{\mathbf{B}} \Theta^*(x, x_0) f_h(x) dV(x) = H_0 (\Theta^*(x_1, x_0) - \Theta^*(x_2, x_0)) \quad (28)$$

$$\iiint_{\mathbf{B}} V_I(x, x_0) f_h(x) dV(x) = H_0 (V_I(x_1, x_0) - V_I(x_2, x_0)) \quad (29)$$

and one obtains truly boundary integral equations, which can be solved with the proposed approach. The results for field intensity factors on inclusion front line are presented in Fig. 3. Normalization factors are equal to $K_{\sigma} = H_0 \beta_{11} \sqrt{\pi} / (k_{11} \sqrt{R})$, $K_{\chi} = H_0 \chi_3 \sqrt{\pi} / (k_{11} \sqrt{R})$, $K_{h0} = -\frac{2H_0}{\sqrt{\pi} R^3}$.

Fig. 3 shows obvious result that for a penny-shaped inclusion ($\rho = 0$) temperature field is not affected ($K_{h2} = 0$), since in the considered symmetric problem $\theta(x_1, x_2, 0) = 0$. Symmetry also causes zero values of the field intensity factor K_{12} in this case. However, due to thermal expansion and pyroelectric effect field intensity factors K_{22} and K_{42} are nonzero. With the increase of inclusion curvature (increase in ρ) field intensity factors increase in their magnitude, and K_{22} even changes its sign. Heat flux intensity factor K_{h2} possesses non-monotonic behavior in its dependence on ρ .

Since the inclusion rotation axis is perpendicular to the material isotropy plane, field intensity factors possess rotational symmetry, and their polar plots are concentric circles (however, due to approximation of the inclusion surface by quadratic boundary elements some of the plots look like polygons; nevertheless, the deviation of the results is less than 0.5%).

References

- [1] **Lopes, V. Jr., Steffen, V. Jr. and Savi, M.A (eds)**: Dynamics of Smart Systems and Structures, *Springer*, London, **2016**.
- [2] **Fang, D. and Liu, J.**: Fracture mechanics of piezoelectric and ferroelectric solids, *Springer*, London, **2013**.
- [3] **Fabrikant, I., Karapetian, E. and Kalinin, S.V.**: Interaction between a punch and an arbitrary crack or inclusion in a transversely isotropic half-space, *Z. Angew. Math. Phys.*, 69, 4, doi: 10.1007/s00033-017-0894-5, **2018**.
- [4] **Kaczyński, A. and Kozłowski, W.**: Thermal stresses in an elastic space with a perfectly rigid flat inclusion under perpendicular heat flow, *International Journal of Solids and Structures*, 46, 1772–1777, **2009**.
- [5] **Kaczyński, A.**: Thermal stress analysis of a three-dimensional anticrack in a transversely isotropic solid, *International Journal of Solids and Structures*, 51, 2382–2389, **2014**.
- [6] **Kaczyński, A.**: On 3D problems of thermoelastostatics for transversely isotropic solids with anticracks, *European Journal of Mechanics / A Solids*, doi: 10.1016/j.euromechsol.2016.01.011, **2016**.
- [7] **Kaczyński, A. and Kaczyński, B.**: On 3D problem of an anticrack under vertically uniform heat flow in a transversely isotropic electro-thermo-elastic space, *European Journal of Mechanics / A Solids*, doi: 10.1016/j.euromechsol.2017.06.004, **2017**.
- [8] **Kirilyuk, V.S.**: Stress state of a piezoceramic body with a plane crack opened by a rigid inclusion, *International Applied Mechanics*, 44, 7, 757–768, **2008**.
- [9] **Pasternak, I., Pasternak, R., Pasternak, V. and Sulym, H.**: Boundary element analysis of 3D cracks in anisotropic thermomagnetoelastic solids, *Engineering Analysis with Boundary Elements*, 74, 70–78, **2017**.
- [10] **Pasternak, I., Pasternak, R. and Sulym, H.**: A comprehensive study on Green's functions and boundary integral equations for 3D anisotropic thermomagnetoelasticity, *Engineering Analysis with Boundary Elements*, 64, 222–229, **2016**.
- [11] **Pasternak, I.**: Coupled 2D electric and mechanical fields in piezoelectric solids containing cracks and thin inhomogeneities, *Engineering Analysis with Boundary Elements*, 35, 678–690, **2011**.
- [12] **Qin, Q.H.**: Green's function and boundary elements of multifield materials, *Elsevier*, Oxford, **2007**.

- [13] **Mi, Y. and Aliabadi, M.H.:** Dual boundary element method for three-dimensional fracture mechanics analysis, *Engineering Analysis with Boundary Elements*, 10, 161–171, **1992**.
- [14] **Dunn, M.L.:** Micromechanics of coupled electroelastic composites: effective thermal expansion and pyroelectric coefficients, *J. Appl. Phys.*, 73, 5131–5140, **1993**.
- [15] **Pasternak, I., Pasternak, R. and Sulym, H.:** Temperature field and heat flux that do not induce stress and electric displacement in a free thermoelectroelastic anisotropic solid, *Mechanics Research Communications*, 57, 40–43, **2014**.

